Goran Gržinić, Thorsten Bartels-Rausch, Mario Birrer, Andreas Türler, and Markus Ammann*

Production and use of ^{13}N labeled N_2O_5 to determine gas–aerosol interaction kinetics

Abstract: Dinitrogen pentoxide has aroused significant interest in atmospheric chemistry because of its importance in the night time chemistry of nitrogen oxides to influence the tropospheric oxidation capacity. We have used an established method of ^{13}N production to synthesize ^{13}N labeled N_2O_5 for the first time in order to study N_2O_5 uptake kinetics on aerosol particles. ^{13}N is produced *via* the $^{16}O(p,\alpha)^{13}N$ reaction in a gas target attached to the IP2 endstation of the Injector 2 cyclotron at PSI. The ^{13}NO produced in the gas target is transported to a laboratory where it is mixed, under dry conditions, with non-labeled NO and O_3 in a gas reactor, giving $^{13}NNO_5$. The N_2O_5 thus produced is fed into an aerosol flow tube together with a humidified aerosol gas flow. The gaseous species present in the resulting gas flow are selectively separated *via* a narrow parallel plate diffusion denuder system, while aerosol particles can be trapped on a particle filter placed at the end of the denuder system. The activity of the ^{13}N labeled species trapped on the denuder plates and in the particle filter can be monitored *via* scintillation counters. A system for the routine online production of ^{13}N labeled N_2O_5 has been assembled and used to assess the conformity of the results by kinetic modeling of gas phase N_2O_5 chemistry, showing good agreement. A few exemplary experiments of uptake of labelled N_2O_5 to ammonium sulfate and citric acid particles are presented that are in good agreement with results obtained with other methods reported in the literature.

Keywords: N_2O_5, Nitrogen-13, Aerosols, Kinetics, Atmospheric Chemistry.

***Corresponding author: Markus Ammann,** Laboratory of Radiochemistry and Environmental Chemistry, Paul Scherrer Institute, 5232 Villigen, Switzerland, e-mail: markus.ammann@psi.ch
Thorsten Bartels-Rausch, Mario Birrer: Laboratory of Radiochemistry and Environmental Chemistry, Paul Scherrer Institute, 5232 Villigen, Switzerland
Goran Gržinić, Andreas Türler: Laboratory of Radiochemistry and Environmental Chemistry, Paul Scherrer Institute, 5232 Villigen, Switzerland; and Department of Chemistry and Biochemistry, University of Bern, 3012 Bern, Switzerland

DOI 10.1515/ract-2014-2244
Received December 20, 2013; accepted June 10, 2014

1 Introduction

During the last two decades the compound N_2O_5 has been the topic of many studies in the field of atmospheric chemistry due to its significant role in the nighttime tropospheric NO_x chemistry. Its formation starts with oxidation of NO_2 to NO_3 radicals by ozone (R1) followed by a reaction with NO_2 that yields N_2O_5 (R2).

$$NO_2 + O_3 \rightarrow NO_3 + O_2 \quad \text{(R1)}$$

$$NO_3 + NO_2 \rightleftarrows N_2O_5 \quad \text{(R2)}$$

Daytime formation of N_2O_5 is inefficient because of the short photolytic lifetime of NO_3 (~1 s); however, during the night N_2O_5 can reach concentrations of up to 10–15 ppb in polluted atmospheres and thus may play an important role in nighttime tropospheric chemistry [1]. During nighttime the concentration of N_2O_5 (as well as NO_3 and NO_2) is controlled by the equilibrium established between N_2O_5 formation and N_2O_5 loss due to thermal decomposition (R2).

The importance of N_2O_5 stems from its role as a NO_3 radical reservoir as well as being a major sink for NO_x species due to the fast heterogeneous hydrolysis reaction with water molecules (R3) on aerosol and ice surfaces [2, 3].

$$N_2O_5 + H_2O \rightarrow 2HNO_3 \quad \text{(R3)}$$

Particle phase nitric acid formed *via* this heterogeneous reaction may then be removed from the atmospheric cycle *via* wet or dry deposition. Due to the equilibrium that exists between NO_2, NO_3 and N_2O_5, removal of the latter reduces the first two which leads to a reduction of tropospheric ozone, thus lowering the oxidizing capacity of the troposphere [1, 4, 5].

Because of the impact of N_2O_5 on ozone formation and the effect that removal *via* hydrolysis on aerosol particles has on the overall budget, uptake kinetics of N_2O_5 on aerosols have been an important topic of study. The

loss rate of N_2O_5 to aerosol particles is determined by the available surface area and the efficiency of the gas phase-aerosol interaction process. It is characterized by the uptake coefficient γ, defined as the probability that a gas kinetic collision of a molecule leads to its uptake at the interface. Studies have been conducted on various types of aerosol particles such as NaCl/sea salt aerosols [6], ammonium sulfate or nitrate particles [7–9], organic aerosols [10], mineral dust [2, 11] and soot [12]. Various detection methods have been used; Cavity Ring-Down Spectroscopy (CRDS) [13] and Chemical Ionization Mass Spectrometry (CIMS) [14] have been particularly popular. CRDS is an optical method that uses a dye laser to inject a laser beam between two mirrors of high reflectivity placed in a cavity. The concentration of the analyte is determined by monitoring the decay of the laser intensity within the cavity with time, the decay rate being directly proportional to the species concentration (in this case NO_3). Thermal conversion of N_2O_5 to NO_3 in a second, heated channel provides simultaneous measurements of the sum of NO_3 and N_2O_5. The method provides very low detection limits (down to the 1–5 pptv range), and allows for parallel measurements of NO_3 and N_2O_5. It can operate at ambient pressure and is relatively compact and thus suitable for field studies. CIMS is based on a selective ionization process resulting from a reaction between a reagent ion and the analyzed species followed by mass spectrometry of the resulting ions. Also this method is highly sensitive (10 pptv range) and the reagent ion used for N_2O_5 studies (I^-) is reasonably specific for either NO_3 or N_2O_5, ionizing both species to NO_3^- detected at 62 amu. The principal drawback of the method is that it cannot differentiate between NO_3 and N_2O_5, and under typical operating conditions often non negligible background noise at 62 amu appears.

While the above mentioned measurement methods have many advantages, they still present some disadvantages that are non negligible, such as difficult operation under high relative humidity or the fact that in laboratory studies N_2O_5 uptake by aerosol particles can only be derived by following its loss from the gas phase. Instead, we have used the short lived ^{13}N radioactive tracer technique developed at the Paul Scherrer Institute [15, 16]. This technique has been used already to study the uptake kinetics of other nitrogen oxides such as HNO_3 [17] and NO_2 [18] to aerosols and of NO_y to ice surfaces [19–21], by labeling them with ^{13}N, a short-lived isotope with a half-life of 10 min. ^{13}N is well known as a positron emitter and also used in positron emission tomography (PET) for medical purposes [22]. In our application, we trace uptake in the particulate phase by monitoring the radioactive decay of ^{13}N labeled N_2O_5 absorbed on aerosol particles while working under realistic ambient temperature and humidity conditions. In this study we will detail the method of production of $^{13}N_2O_5$ and the experimental setup to study the uptake kinetics on aerosol particles as well as report a few exemplary measurements on aerosol particles to benchmark against other methods. To our knowledge this is the first time that ^{13}N labeled N_2O_5 has been produced for experimental purposes.

2 Experimental

2.1 General layout of the experiment

Using the shortlived radioactive tracer ^{13}N allows for the study of heterogeneous kinetics under realistic conditions, and experiments can be performed at very low trace gas concentrations (down to a hundred pptv) and in presence of high relative humidity. ^{13}N labeled NO is mixed with O_3 in a first reactor to produce $^{13}N_2O_5$, which is then fed into an aerosol flow tube where it can be mixed with aerosols to perform heterogeneous kinetics experiments. The result-

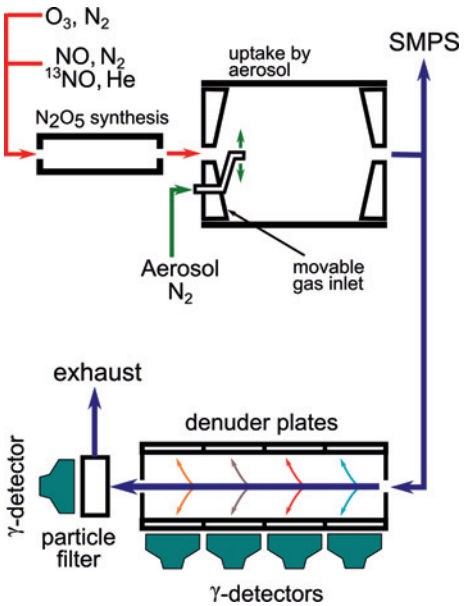

Fig. 1: Schematic representation of the experimental arrangement. N_2O_5 is synthesized in the first reactor. Mixing with aerosol is achieved in an aerosol flow tube with movable inlets which allows to adjust the reaction time. The resulting gas flow is directed into the paralel plate denuder system where 4 sets of plates covered with denuder coatings (citric acid and NDA) are used to selectively separate the gas phase products. The particle phase products are trapped on the particle filter. Gamma detectors are used to monitor the activity of the products. SMPS denotes the scanning mobility particle sizer.

ing flow is then directed into a parallel plate diffusion denuder system where the gaseous and particle phase products can be selectively separated and trapped on coated denuder plates and a particle filter, respectively. By monitoring the decay of ^{13}N on each trap it is possible to derive simultaneously the concentration of the various ^{13}N labeled species in the gas and particle phase. Figure 1 shows a schematic diagram of our experimental arrangement.

2.2 Production and transport of ^{13}NO

At the Paul Scherrer Institute ^{13}NO has been produced for the purpose of tracer experiments in atmospheric chemistry since about two decades. A detailed description of the method has been described earlier [15]. Briefly, ^{13}N is produced *via* the $^{16}O(p,\alpha)^{13}N$ reaction in a gas-target by irradiating ^{16}O with about 11 MeV protons at around 10 μA intensity. Developed from an earlier design [15], the gas-target is a conically shaped aluminium flow reactor attached to the Isotope Production Station IP2 at a branch of the Injector II cyclotron at PSI. The primary proton beam with an energy of 72 MeV is passed through a first degrader to bring the energy down to 35 MeV. The window into the ^{13}N target, consisting of two water cooled aluminium windows, is designed such that the energy of the protons at the entry into the gas volume is further degraded down to about 11 MeV. The further degradation within the gas target depends on pressure, which was kept at 2.5 bar, and a continuous 1 l/min STP flow of 20% O_2 in He (all flow rates are given in volumetric flow normalized to standard temperature and pressure) is passed through the target. This pressure was also constrained by other boundary conditions of our experiments and not adjusted to optimize ^{13}N production according to the detailed structure of the excitation function for the $^{16}O(p,\alpha)^{13}N$ reaction [23, 24]. Highly oxidized and reactive forms of nitrogen oxides are produced and chemically converted to ^{13}NO over a Mo converter (at ~380 °C) connected to the gas-target in order to facilitate transport. As discussed in our earlier study [15], quantitative ^{13}N output is difficult to achieve, likely due to chemical losses on surfaces before the Mo converter. Non-labeled nitrogen oxide species (at around 8 ppbv) are also produced from nitrogen impurities in the carrier gas and likewise converted to NO. Only a very small fraction of the overall NO produced contain the tracer atoms (below ppt levels), Additionally, trace amounts of carbon monoxide or carbon dioxide are formed from organic impurities present in the gas feed. The resulting ^{13}NO containing gas is then continuously transported to the laboratory *via* a 580 m long PVDF tube (inner diameter 4 mm).

2.3 Production of $^{13}N_2O_5$

In the laboratory, selected amounts of the target gas flow (typically 50 ml/min) can be mixed with variable amounts of N_2 and certified amounts (1 ml/min) of non-labeled NO from a gas cylinder (10 ppm in N_2) allowing to cover a wide range of NO concentrations in the ppb range. Possible traces of HONO are removed by using a Na_2CO_3 trap.

The ^{13}NO gas flow is directed into the N_2O_5 reactor where it is mixed with a flow (50 ml/min) containing ozone (~4 ppmv in this reactor) in order to generate ^{13}N labeled N_2O_5 *via* reactions (R1) and (R2). O_3 is produced by passing a flow of 10% O_2 in N_2 over a UV lamp (185 nm wavelength). The N_2O_5 reactor is covered with a shroud in order to prevent NO_3 photolysis and thus loss of N_2O_5. Additionally, in order to minimize losses due to heterogeneous hydrolysis on the walls, N_2O_5 production is conducted under dry conditions, and the walls of the reactor are covered with PTFE foil. The resulting gas flow (101 ml/min) is then fed into the flow tube reactor, where it is mixed with the aerosol flow (720 ml/min).

2.4 Modeling of gas phase $^{13}N_2O_5$ production

As a support tool for the design of the experiment and to address issues such as the slow formation of N_2O_5 *via* reactions (R4), (R1) and (R2) *vs.* the radioactive decay of ^{13}N with a half-life of 10 min, a modeling study of gas phase N_2O_5 formation has been carried out. The kinetics was based on the recommendations of the IUPAC Task Group on Atmospheric Chemical Kinetic Data Evaluation [25] and the NASA Panel for Data Evaluation [26]. Modeling work has been performed in Matlab using ODE (ordinary differential equation) solvers and using temperature, pressure, time, reactor geometry and starting concentrations for NO and O_3 as input variables. Wall loss was also incorporated into the model. Overall 12 reactions have been included in the model (R4–R15). The rate coefficients listed beside the reactions are given at standard temperature and pressure. In the computer model pressure and temperature dependence of the rate coefficients as recommended in the above mentioned data bases has been included.

$$NO + O_3 \longrightarrow NO_2 + O_2 \qquad k = 1.8 \times 10^{-14}\ \mathrm{cm^3\ molecule^{-1}\ s^{-1}} \qquad \text{(R4)}$$

$$NO_2 + O_3 \longrightarrow NO_3 + O_2$$
$$k = 3.5 \times 10^{-17}\ \mathrm{cm^3\ molecule^{-1}\ s^{-1}} \quad \text{(R5)}$$

$$NO_2 + NO_3 \xrightarrow{M} N_2O_5$$
$$k = 8.8 \times 10^{-11}\ \mathrm{cm^3\ molecule^{-1}\ s^{-1}} \quad \text{(R6)}$$

$$N_2O_5 \xrightarrow{M} NO_2 + NO_3$$
$$k = 6.9 \times 10^{-2}\ \mathrm{s^{-1}} \quad \text{(R7)}$$

$$2NO + O_2 \longrightarrow 2NO_2$$
$$k = 2.0 \times 10^{-38}\ \mathrm{cm^6\ molecule^{-2}\ s^{-1}} \quad \text{(R8)}$$

$$NO + NO_2 \xrightarrow{M} N_2O_3$$
$$k = 7.66 \times 10^{-15}\ \mathrm{cm^3\ molecule^{-1}\ s^{-1}} \quad \text{(R9)}$$

$$N_2O_3 \xrightarrow{M} NO + NO_2$$
$$k = 3.6 \times 10^{8}\ \mathrm{s^{-1}} \quad \text{(R10)}$$

$$NO + NO_3 \longrightarrow 2NO_2$$
$$k = 2.6 \times 10^{-11}\ \mathrm{cm^3\ molecule^{-1}\ s^{-1}} \quad \text{(R11)}$$

$$2NO_2 \xrightarrow{M} N_2O_4$$
$$k = 1.0 \times 10^{-12}\ \mathrm{cm^3\ molecule^{-1}\ s^{-1}} \quad \text{(R12)}$$

$$N_2O_4 \xrightarrow{M} 2NO_2$$
$$k = 4.4 \times 10^{6}\ \mathrm{s^{-1}} \quad \text{(R13)}$$

$$NO_2 + NO_3 \longrightarrow NO + NO_2 + O_2$$
$$k = 6.76 \times 10^{-16}\ \mathrm{cm^3\ molecule^{-1}\ s^{-1}} \quad \text{(R14)}$$

$$2NO_3 \longrightarrow 2NO_2 + O_2$$
$$k = 2.42 \times 10^{-16}\ \mathrm{cm^3\ molecule^{-1}\ s^{-1}} \quad \text{(R15)}$$

The model allowed us to analyze the influence of O_3 and NO concentrations on N_2O_5 production and its temperature dependence as well as estimating the N_2O_5/NO_3 ratio in the gas phase. The resulting estimates and predictions were used in the experimental design phase to optimize the production of N_2O_5 as well as to benchmark our N_2O_5 production process to the known gas phase kinetic data.

2.5 Aerosol generation and characterization

The aerosol was produced by nebulizing a 0.7% (by weight) solution of citric acid (HQ, Fluka, >99%) or of 0.69% wt. solution of ammonium sulfate in MilliQ water by means of an ultrasonic nebulizer. Citric acid was used as a proxy for a generic organic aerosol while ammonium sulfate was chosen because of the wealth of experimental data already available in the literature. The mist droplets formed were dried by passing the flow through a Nafion membrane diffusion dryer. The sheath gas outside the Nafion membrane was humidified such that the resulting aerosol flow had the relative humidity intended for the experiment by avoiding efflorescence of the particles in experiments below the deliquescence relative humidity. In order to avoid uncontrolled losses of charged aerosol particles to the insulating walls of tubing and the aerosol flow reactor, the aerosol flow was passed through a ^{85}Kr ion source, to establish an equilibrium charge distribution, followed by an electrostatic precipitator removing all charged particles. After that the aerosol flow was fed into the aerosol flow tube.

When aerosol was used in the experiments, measurement of its surface area to gas volume ratio was performed with a Scanning Mobility Particle Sizer (SMPS). This system consists of a homemade ^{85}Kr source to establish charge equilibrium of the aerosol, a differential mobility analyzer (DMA, TSI 3071) and a condensation particle counter (CPC, TSI 3022). Since the aerosol water content and consequently the particle diameter and aerosol surface to volume ratio strongly depend on relative humidity, filtered carrier gas from the flow tube was used as sheath gas in the DMA in order to keep the two flows in equilibrium. Aerosol sampling was conducted at an outlet directly behind the aerosol flow tube, where additionally other instruments such as NO_x or O_3 analyzers could be connected as well.

2.6 Aerosol flow tube

The aerosol and N_2O_5 containing gas flow were mixed together in the cylindrical aerosol flow tube composed of a PFA tube with an inner diameter of 7 cm and a movable inlet and outlet that allow adjusting the length of the aerosol – gas interaction zone and thus the reaction time inside the flow tube. The gas flow is introduced *via* a conically shaped gas inlet along the axis of the flow tube. The aerosol flow is introduced into the flow tube *via* a fixed injector which protrudes from the side of the conical inlet. The injector is a 6 mm diameter Inox steel tube bent in such a way that the injector nozzles are equidistant from the reactor walls and the aerosol flow is injected perpendicularly to the gas flow. When the outlet is pushed all the way in to the minimum position inside the flow tube, the reaction time is minimum (~10 s), while pulling the outlet to the maximum position one can achieve a reaction time of 60 s. The flow tube is operated under laminar flow conditions and it is assumed that a laminar flow profile is established a few cm downstream of the aerosol injector. PFA has been chosen in an attempt to minimize N_2O_5 losses to the wall. While losses are lower than with a glass tube reac-

tor, they are still substantial when operating under humid conditions.

2.7 Detection system

Following the aerosol flow tube, the combined gas flow was directed towards the parallel plate diffusion denuder system. A T-connector was placed between the two in order to allow connecting the SMPS system or a NO_x or O_3 detector. Upon entering the denuder train the gaseous species (N_2O_5 and NO_2) are separated on different chemically selective coatings by lateral diffusion. The sub-micron aerosol particles have a small diffusivity and pass through the denuder unobstructed with almost 100% efficiency. Gaseous N_2O_5 (and the small amounts of NO_3 present) was collected on the first set of denuder plates coated with citric acid, prepared from a 2 wt % solution in 50% methanol/water. Citric acid has well documented hygroscopic properties [27] and mixes well with water, thus facilitating coating preparation. It also forms a solution down to low relative humidity and thus maintains reactivity also in experiments at low relative humidity. The citric acid coating was applied to the first and second denuder plate set; the former to capture N_2O_5, the latter to monitor the interference of NO_2 on the citric acid coating. The third and fourth sets of denuder plates were coated with NDA (N-(1-naphtyl) ethylene diamine dihydrochloride) mixed with KOH (1% solution with 1% KOH and 10% water in methanol). NDA absorbs NO_2 very efficiently and the basic coating assures that the nitrite product stays on the surface. Two denuder plate sets with NDA were used, because NDA is sensitive to ozone present in our system and is depleted rapidly, so the second denuder plate is used to extend the available experimental time. Fresh coatings were prepared and applied every day. After passing the denuder system, the aerosol particles were captured by a glass fiber filter. ^{13}N decay results in the emission of a positron, which, upon annihilation with an electron, results in the coincident emission of two γ-rays in opposite directions. To each trap (the coatings and filter) a separate CsI scintillator crystal with integrated PIN diode detector was attached (Carroll and Ramsey, USA), which detects the gamma quanta emitted after decay of the ^{13}N atoms. The detector signal is converted to the flux of the gaseous species into the trap using the inversion procedure reported earlier [16, 28]. This flux is proportional to the concentration of the species in the gas phase. The relative counting efficiency of the various γ-detectors was determined by exposing in turn each of the detectors to a glass fiber filter on which a drop of a ^{22}NaI solution was deposited, in a way that closely mimics the geometrical configuration at each trap. Additional information about coating preparation, traps and measurement efficiencies can be found elsewhere [15, 16].

3 Results and discussion

3.1 Gas phase production of $^{13}N_2O_5$

Our experiments dealing with production of $^{13}N_2O_5$ were conducted with a 4 min residence time in the N_2O_5 reactor and 1 min residence time in the aerosol flow tube in order to simulate default operating settings also used for the aerosol experiments reported further below. These settings resulted in an NO concentration of 99 ppbv and an O_3 concentration of ~4 ppmv in the N_2O_5 reactor. The resulting gas flow was fed into the flow tube, together with the flow from the aerosol gas line. The ultrasonic nebulizer connected to this gas flow line was turned off (and thus no aerosol was generated) since only gas phase kinetics were studied in this step. The humidity inside the aerosol flow tube was kept at ~27% RH (humidified aerosol gas flow). Figure 2 shows the resulting N_2O_5 and NO_2 gas phase signals measured at the parallel plate diffusion denuder system.

N_2O_5 and NO_3 are absorbed on the first denuder plate set coated with citric acid. The second citric acid coated plate set, which is placed after the first, shows the NO_2 interference signal on the citric acid coating. Finally, the NDA coated denuder plate set gives the NO_2 signal. When ^{13}NO and non labeled NO were fed into the system (12:46), the activity on all coatings increased. The signals originate from the background of ^{13}NO decaying in the gas phase while passing through the denuder system and the filter and from small amounts of $^{13}NO_2$ and $HO^{13}NO$ formed along the flow system that were trapped in the first citric acid coating. When O_3 was turned on for the first time a marked increase of the signal on the first citric acid denuder plate set occurred due to N_2O_5 (and NO_3, see below) that was formed. The signal derived from the second citric acid plate set shows a modest increase that is due to the NO_2 interference on the citric acid coating. Lastly, the NO_2 signal shows a significant increase due to its formation from NO and O_3. When O_3 was turned off, the N_2O_5 signal dropped rapidly while the other two signals did so gradually. The dynamic response of the NO_2 signal in between is discussed below. The certified NO flow was then doubled to 2 ml/min (14:23, 196 ppbv in N_2O_5 reactor) and O_3 was turned on again. The signals have a behavior similar to the earlier ones, but with an increase in lev-

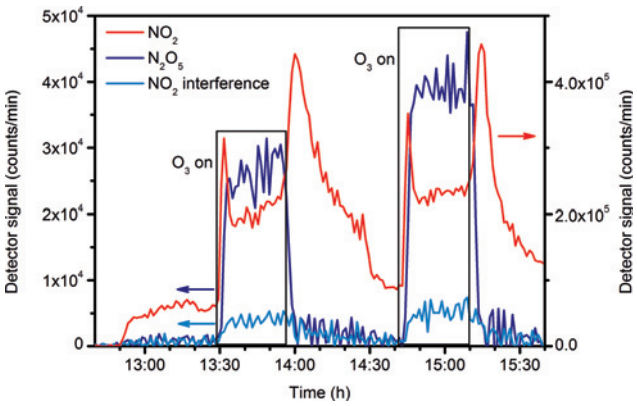

Fig. 2: Production of gas phase $^{13}N_2O_5$: dark blue: first citric acid denuder signal (gas phase N_2O_5); light blue: second citric acid denuder signal (NO_2 interference on citric acid denuder); red: NDA denuder signal (gas phase NO_2).

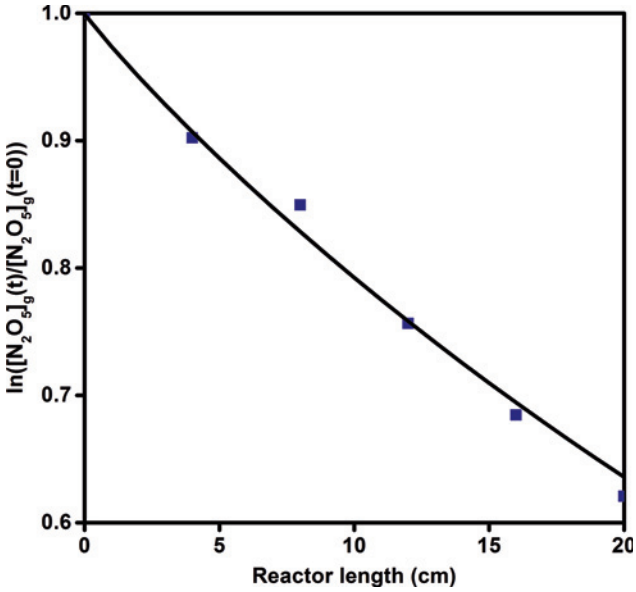

Fig. 3: Decay plot of N_2O_5 *vs.* reactor length fitted to the measured data using the CKD method.

els that can be attributed to the higher NO concentration (see model calculations below). The plotted signals also give some indication of the transient behavior of the gas phase system. In particular, peaks in the NO_2 signal can be noticed shortly after O_3 was turned on and off. This is due to the kinetics of the reactions involved and in particular (R1), (R2) and (R4). When O_3 was turned on we observed the fast titration of NO to yield NO_2 (R4). The subsequent reaction of NO_2 with O_3 to give NO_3 (R1) is about 3 orders of magnitude slower than (R4). As NO_2 was transformed into NO_3 the NO_2 signal diminished until it reached a steady-state level. When O_3 was turned off, the faster reaction R4 consumed the remaining O_3 to effectively suppress reaction R1 and thus NO_2 was no longer converted to NO_3. This brought about another increase of the NO_2 signal before it gradually decreased as the rest of the O_3 was consumed.

3.2 Comparison with model

In order to obtain a quantitative value for the N_2O_5 signal measured at the parallel plate denuder system we connected a NO_x analyzer (ML 9841A) at the T connector behind the aerosol flow tube reactor. In this way we were able to measure the NO_2 concentration in the system and consequently calculate the N_2O_5 concentration in the gas and particle phase from the $^{13}NO_2$ and $^{13}N_2O_5$ signals observed on the denuder plates and particle filter. Thus we were able to calibrate the setup and assign a concentration value to the denuder plate and particle filter signals.

The next step in the process was to evaluate the wall loss in the aerosol flow tube. The wall uptake represents the loss of gas phase N_2O_5 due to hydrolysis on the walls of the flow tube. Measurements were performed by varying the flow tube length (residence time) and measuring the gas phase N_2O_5 concentration in the reactor at each length. Flow tube lengths from 0 cm (10 s) to 20 cm (60 s) were evaluated, using the 10 s position as the starting point as shown in the resulting decay plot (Figure 3).

The measured, pseudo-first order loss rate constant k_{wall} was determined to be equal to 9.5×10^{-3} s^{-1}, giving an effective coefficient of uptake on the wall (γ_{wall}) of 2.8×10^{-6}. A correction of the observed uptake rate for diffusion in the gas phase using the Cooney-Kim-Davis (CKD) method was applied [29], which yielded an uptake coefficient of 3.7×10^{-6}.

Finally, a data comparison of N_2O_5 formation from NO and O_3 with the model calculation was performed. First, a model calculation was made for the N_2O_5 reactor using the initial NO and O_3 concentrations therein. The resulting gas phase concentrations obtained from the model (Figure 4a) were then corrected for dilution by the aerosol flow into the aerosol flow tube. The model calculations were then performed again, this time for the aerosol flow tube, taking into account the experimentally measured k_{wall} (Figure 4b). Thus the whole experimental system can be accounted for (N_2O_5 reactor+flow tube reactor) and modeled as a single entity. The experimental results appear in good agreement with the data obtained from model calculations, although the expected concentrations were slightly lower than the measured ones. Note that the slope was constrained by the k_{wall} measurement

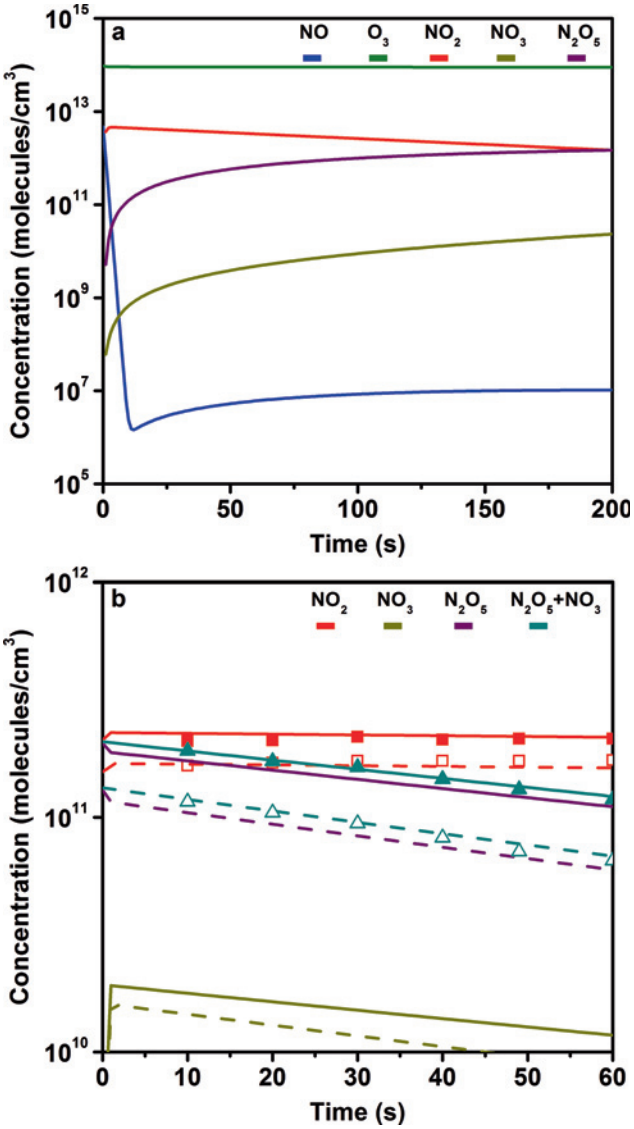

Fig. 4: Gas phase model graphs: (a) N_2O_5 reactor with residence time of 195 sec; (b) flow tube reactor with residence time of 60 sec (calculated using the measured k_{wall}). Full lines represent modeled values using 196 ppb initial NO concentration, dashed lines using 148 ppb initial NO concentration. The data points represent measured values using initial NO concentrations of 196 ppb (full points) and 148 ppb (open points).

and thus consistency of the modeled slope with the measured slope for N_2O_5 with time is not surprising. However, the model estimates the absolute concentration level fairly well. The difference between model and measurement is probably at least in part due to the value of k_{wall} (and γ_{wall} respectively) for the N_2O_5 reactor that we used in the model calculations and that remained an adjustable parameter. It should be noted that, as mentioned in the experimental section, it is not possible to distinguish between N_2O_5 and NO_3 in the gas phase since both are taken up efficiently on the denuder coating. The contribution of NO_3 to the overall signal depends primarily on temperature, since the decomposition of N_2O_5 to its precursors is a thermally driven process. At STP the NO_3 concentration is roughly one order of magnitude lower than that of N_2O_5. Figure 4b shows this contribution.

The uptake coefficient on the wall for the N_2O_5 reactor was not measured; however, taking into consideration the values obtained for the aerosol flow tube and the fact that N_2O_5 synthesis is performed under dry conditions, a conservative value in the range of $1–5 \times 10^{-7}$ has been assumed by fitting the model to the experimental data. As mentioned above, this has given good results. Changing the value to 10^{-8} gives N_2O_5 levels slightly above those measured, while the NO_2 levels show negligible changes. On the other hand, when using a value of 10^{-6}, the N_2O_5 level is lower by roughly a factor of two compared to measured results, while the NO_2 levels decrease as well, albeit not so strongly. As far as the aerosol flow tube is concerned, increases in γ_{wall} and k_{wall} (for example in cases of higher humidity) bring about a strong drop in N_2O_5 levels, while NO_2 levels show negligible changes.

3.3 Uptake by aerosol

An exemplary measurement of ^{13}N labeled N_2O_5 uptake by citric acid aerosol particles at 27% relative humidity and a N_2O_5 concentration of ~5 ppbv is shown in Figure 5. When aerosol was fed into the system by switching on the ultrasonic nebulizer, uptake was observed by measuring an increase in activity on the particle filter. At the same time the gas phase N_2O_5 signal slightly decreased, corresponding to a drop in gas phase concentration by 0.31 ppbv. However the resulting aerosol signal accounts for only 0.16 ppbv lost from the gas phase. This is the result of the complex interplay of wall loss and uptake by the particles under conditions where the apparent wall loss is larger than the loss to the particles.

By applying the principles of gas-aerosol interaction kinetics (E1), we can analyze the net uptake kinetics from the signal in the aerosol phase and the measured wall loss rate constant in absence of aerosol.

$$\frac{C_p^{(t)}}{C_p^{(t=0)}} = \frac{1 - e^{-(k_w+k_p)t}}{1 + \frac{k_w}{k_p}} \qquad \text{(E1)}$$

where $C_g^{(t=0)}$ is the initial gas-phase concentration of N_2O_5 at time zero, $C_p^{(t)}$ is the concentration of N_2O_5 in the particulate phase, k_p is the constant for the heterogeneous reaction between gaseous N_2O_5 acid and aerosol

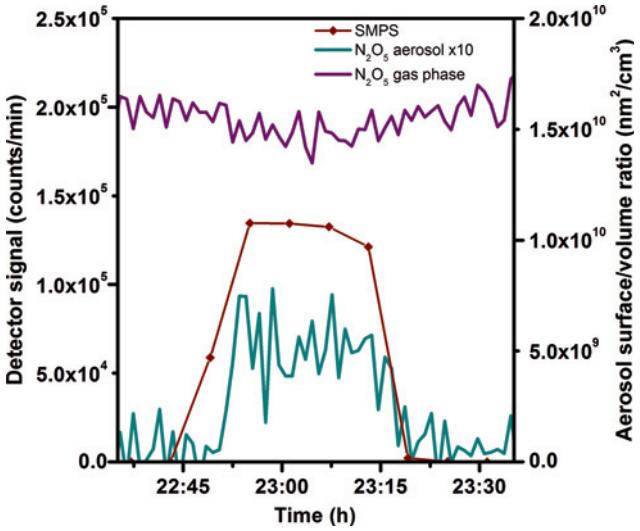

Fig. 5: N_2O_5 interacting with citric acid aerosol (295 K, 26% RH): purple: first citric acid denuder signal (gas phase N_2O_5); dark yellow: signal from particle filter multiplied by a factor of 10 (particle phase N_2O_5 or nitrate); dark red: SMPS signal (aerosol surface/volume ratio).

particles and k_w describes the N_2O_5 loss to the wall [16]. The heterogeneous rate constant k_p is related to the uptake coefficient γ according to E2:

$$\gamma = \frac{4k_p}{S_p\omega} \qquad \omega = \sqrt{\frac{8RT}{\pi M}} \tag{E2}$$

where S_p is the aerosol surface to volume ratio, ω is the mean thermal velocity of N_2O_5, R is the gas constant, T is the absolute temperature and M is the molar weight of N_2O_5.

In the experiments that were conducted, the surface to volume ratio of the aerosol was varied by changing the settings at the ultrasonic nebulizer. From the obtained experimental data the value of the uptake coefficient for citric acid at 27% RH has been estimated at $1.4 \pm 0.4 \times 10^{-3}$.

An experiment was also conducted using ammonium sulphate aerosol at 52% relative humidity (Figure 6). It becomes immediately apparent that the signal on the particles scales with the aerosol surface area. Since this experiment has been performed at higher humidity than the one with citric acid shown above, the background signal of N_2O_5 in absence of aerosol is lower due to a larger value of k_{wall}. Surprisingly, we observe a small but significant increase in the N_2O_5 (g) signal in presence of aerosol. The characteristic gas – aerosol separation time in the denuder is about 30 ms per pair of coated plates. Since the time scale for diffusion of a dissolved species through the submicron particles is on the order of microseconds, there is enough time for any dissolved N_2O_5 to escape and being trapped. However, we also see a corresponding increase of the signal in the second pair of denuder plates we use for assessing the NO_2 interference. This indicates that there is also a slow process leading to evaporation of N_2O_5. The fate of dissolved N_2O_5 is the disproportionation into NO_2^+ and NO_3^-. It is therefore likely that the slow evaporation of N_2O_5 out of the particles over time scales of about 100 ms or more may be limited by the kinetics of the back reaction of NO_2^+ and NO_3^-. There is also the possibility that HNO_3, the product of N_2O_5 uptake, is evaporating from the particles [9, 30]. In spite of its strong degree of dissociation, a small amount of undissociated HNO_3 exists within the particles that remains in equilibrium with the gas phase. However, we would expect that stripping off excess HNO_3 would only be limited by the time scale of diffusion through the particles, which is on the order of microseconds. The fact that the increase in signal also occurs on the second citric acid coating could thus only result from additional HNO_3 formed from the reaction of NO_2^+ with water after passing through the first denuder plate set, the extent of which is in turn again limited by how long NO_2^+ remains available before being converted back to N_2O_5.

Using the data obtained we calculated the uptake coefficient for ammonium sulphate at 52% RH, which is equal to $1.45 \pm 0.35 \times 10^{-2}$. This is in excellent agreement with previously reported results [31].

As can be seen in Figure 6, the particle signal in the case of ammonium sulphate is stronger than in the case of citric acid. This is consistent with the increased water content in ammonium sulphate vs. citric acid aerosol (40 vs. 10 M) as calculated using the Extended AIM Aerosol Thermodynamics Model [32] and a parameterization of the hygroscopic studies of citric acid [33]. Assuming that the Henry's Law coefficient (H) does not change with the ionic strength of the solution, the increased water content increases the amount of dissolved N_2O_5, and thus also the extent of the reversible disproportionation reaction of dissolved N_2O_5 with water to give NO_2^+ and NO_3^- in the aerosol phase. In turn, this leads to an increased extent of reaction of NO_2^+ with water and thus increased net uptake of N_2O_5 from the gas phase.

4 Conclusions and outlook

We have produced ^{13}N labeled N_2O_5 for the first time. An experimental setup has been assembled for the study of uptake kinetics of N_2O_5 on aerosol particles and has been successfully tested. Gas phase N_2O_5 production data has

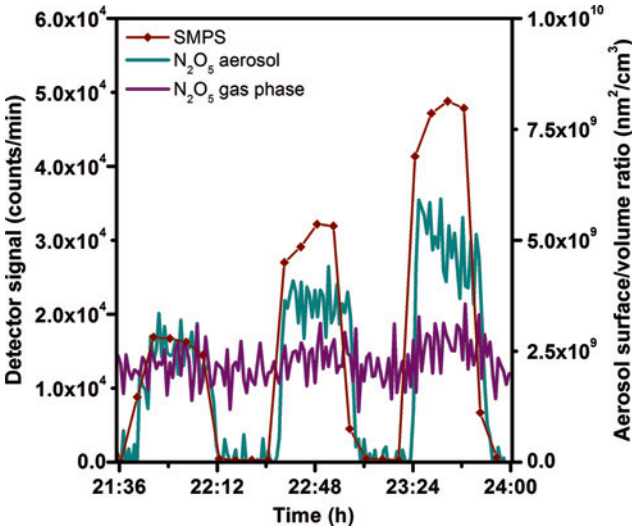

Fig. 6: N_2O_5 interacting with ammonium sulphate particles at different aerosol S/V ratios (295 K, 52% RH): purple: first citric acid denuder signal (gas phase N_2O_5); dark yellow: signal from particle filter (particle phase N_2O_5 or nitrate); dark red: SMPS signal (aerosol surface/volume ratio).

shown good agreement with results obtained with a kinetic model. Measured data has shown that the experimental method also gives insight into the dynamics of the gas phase system. Routine production of N_2O_5 in the ppb range has been achieved, allowing for further studies involving ^{13}N labeled N_2O_5.

Additionally, aerosol uptake experiments were conducted in order to test the experimental setup under realistic conditions. Uptake on citric acid aerosol has been observed and quantified. Uptake on ammonium sulphate aerosol has likewise been observed and an uptake coefficient has been measured that is consistent with that reported in the literature for deliquesced ammonium sulphate. Since the method allows tracing uptake in the particulate phase, this opens the way for further experiments with other types of aerosols at a wider range of humidities as well as temperatures. Of particular interest would be the possibility to monitor the exchange with the particulate nitrate pool in nitrate aerosols.

Overall the study has shown the viability of the proposed method to produce ^{13}N labeled N_2O_5 for atmospheric science related experimental studies, and in particular the assembled setup and the related operating procedures will be used in future studies of N_2O_5 uptake kinetics on aerosol particles.

Acknowledgement: The authors would like to thank the staff of the PSI accelerator facilities and of the isotope production facility IP-2 for their invaluable help. This work is supported by the Swiss National Science Foundation (grant no. 130175).

References

1. Finlayson-Pitts, B. J., Pitts Jr., J. N.: *Chemistry of the upper and lower atmosphere*, Academic Press, San Diego 2000.
2. Wagner, C., Hanisch, F., Holmes, N., de Coninck, H., Schuster, G., Crowley, J. N.: The interaction of N_2O_5 with mineral dust: aerosol flow tube and Knudsen reactor studies. Atmos. Chem. Phys. **8**(1), 91–109 (2008).
3. Chang, W. L., Bhave, P. V., Brown, S. S., Riemer, N., Stutz, J., Dabdub, D.: Heterogeneous atmospheric chemistry, ambient measurements, and model calculations of N(2)O(5): a review. Aerosol Sci. Technol. **45**(6), 665–695 (2011).
4. Dentener, F. J., Crutzen, P. J.: Reaction of N_2O_5 on tropospheric aerosols: impact on the global distributions of NO_x, O_3 and OH. J. Geophys. Res. **98**(D4), 7149–7163 (1993).
5. Evans, M. J., Jacob, D. J.: Impact of new laboratory studies of N_2O_5 hydrolysis on global model budgets of tropospheric nitrogen oxides, ozone and OH. Geophys. Res. Lett. **32**(9), L09813 (2005).
6. Thornton, J. A., Abbatt, J. P. D.: N_2O_5 reaction on submicron sea salt aerosol: kinetics, products, and the effect of surface active organics. J. Phys. Chem. A **109**(44), 10004–10012 (2005).
7. Badger, C. L., Griffiths, P. T., George, I., Abbatt, J. P. D., Cox, R. A.: Reactive uptake of N_2O_5 by aerosol particles containing mixtures of humic acid and ammonium sulfate. J. Phys. Chem. A **110**(21), 6986–6994 (2006).
8. Wagner, R., Naumann, K. H., Mangold, A., Mohler, O., Saathoff, H., Schurath, U.: Aerosol chamber study of optical constants and N_2O_5 uptake on supercooled $H_2SO_4/H_2O/HNO_3$ solution droplets at polar stratospheric cloud temperatures. J. Phys. Chem. A **109**(36), 8140–8148 (2005).
9. Wahner, A., Mentel, T. F., Sohn, M., Stier, J.: Heterogeneous reaction of N_2O_5 on sodium nitrate aerosol. J. Geophys. Res.-Atmos. **103**(D23), 31103–31112 (1998).
10. Griffiths, P. T., Badger, C. L., Cox, R. A., Folkers, M., Henk, H. H., Mentel, T. F.: Reactive uptake of N_2O_5 by aerosols containing dicarboxylic acids. effect of particle phase, composition, and nitrate nontent. J. Phys. Chem. A **113**(17), 5082–5090 (2009).
11. Tang, M. J., Thieser, J., Schuster, G., Crowley, J. N.: Kinetics and mechanism of the heterogeneous reaction of N_2O_5 with mineral dust particles. Phys. Chem. Chem. Phys. **14**(24), 8551–8561 (2012).
12. Karagulian, F., Rossi, M. J.: Heterogeneous chemistry of the NO_3 free radical and N_2O_5 on decane flame soot at ambient temperature: reaction products and kinetics. J. Phys. Chem. A **111**(10), 1914–1926 (2007).
13. Brown, S. S., Dube, W. P., Fuchs, H., Ryerson, T. B., Wollny, A. G., Brock, C. A., Bahreini, R., Middlebrook, A. M., Neuman, J. A., Atlas, E., Roberts, J. M., Osthoff, H. D., Trainer, M., Fehsenfeld, F. C., Ravishankara, A. R.: Reactive uptake coefficients for N_2O_5 determined from aircraft measurements during the Second Texas Air Quality Study: comparison to current model parameterizations. J. Geophys. Res.-Atmos. **114**(D7), D00F10 (2009).

14. Gross, S., Iannone, R., Xiao, S., Bertram, A. K.: Reactive uptake studies of NO_3 and N_2O_5 on alkenoic acid, alkanoate, and polyalcohol substrates to probe nighttime aerosol chemistry. Phys. Chem. Chem. Phys. **11**(36), 7792–7803 (2009).
15. Ammann, M.: Using ^{13}N as tracer in heterogeneous atmospheric chemistry experiments. Radiochim. Acta **89**, 831–838 (2001).
16. Guimbaud, C., Arens, F., Gutzwiller, L., Gaggeler, H. W., Ammann, M.: Uptake of HNO_3 to deliquescent sea-salt particles: a study using the short-lived radioactive isotope tracer N-13. Atmos. Chem. Phys. **2**, 249–257 (2002).
17. Vlasenko, A., Sjogren, S., Weingartner, E., Stemmler, K., Gäggeler, H. W., Ammann, M.: Effect of humidity on nitric acid uptake to mineral dust aerosol particles. Atmos. Chem. Phys. **6**, 2147–2160 (2006).
18. Sosedova, Y., Rouvière, A., Gäggeler, H. W., Ammann, M.: Uptake of NO_2 to deliquesced dihydroxybenzoate aerosol particles. J. Phys. Chem. A **113**, 10979–10987 (2009).
19. Bartels-Rausch, T., Eichler, B., Zimmermann, P., Gäggeler, H. W., Ammann, M.: The adsorption of nitrogen oxides on crystalline ice. Atmos. Chem. Phys. **2**(3), 235–247 (2002).
20. Bartels-Rausch, T., Ulrich, T., Huthwelker, T., Ammann, M.: A novel synthesis of the N-13 labeled atmospheric trace gas peroxynitric acid. Radiochim. Acta **99**(5), 285–292 (2011).
21. Ulrich, T., Ammann, M., Leutwyler, S., Bartels-Rausch, T.: The adsorption of peroxynitric acid on ice between $230\ K$ and $253\ K$. Atmos. Chem. Phys. **12**(4), 1833–1845 (2012).
22. Miller, P. W., Long, N. J., Vilar, R., Gee, A. D.: Synthesis of C-11, F-18, O-15, and N-13 radiolabels for positron emission tomography. Angew. Chem.-Int. Edit. **47**(47), 8998–9033 (2008).
23. Sajjad, M., Lambrecht, R. M., Wolf, A. P.: Cyclotron isotopes and radiopharmaceuticals .37. Excitation-functions for the O-16(p, α)N-13 and N-14(p, pn)N-13 reactions. Radiochim. Acta **39**(3), 165–168 (1986).
24. Qaim, S. M.: Nuclear data relevant to the production and application of diagnostic radionuclides. Radiochim. Acta **89**(4–5), 223–232 (2001).
25. Atkinson, R., Baulch, D. L., Cox, R. A., Crowley, J. N., Hampson, R. F., Hynes, R. G., Jenkin, M. E., Rossi, M. J., Troe, J.: Evaluated kinetic and photochemical data for atmospheric chemistry: Volume I – gas phase reactions of O_x, HO_x, NO_x and SO_x species. Atmos. Chem. Phys. **4**(6), 1461–1738 (2004).
26. Sander, S. P., Abbatt, J., Barker, J. R., Burkholder, J. B., Friedl, R. R., Golden, D. M., Huie, R. E., Kolb, C. E., Kurylo, G. M. J., Moortgat, K., Orkin, V. L., Wine, P. H.: Chemical kinetics and photochemical data for use in atmospheric studies, Evaluation no. 17. JPL Publication, Jet Propulsion Laboratory, Pasadena, USA **10**(6) (2011).
27. Peng, C., Chan, M. N., Chan, C. K.: The hygroscopic properties of dicarboxylic and multifunctional acids: measurements and UNIFAC predictions. Environ. Sci. Technol. **35**(22), 4495–4501 (2001).
28. Kalberer, M., Tabor, K., Ammann, M., Parrat, Y., Weingartner, E., Piguet, D., Rossler, E., Jost, D. T., Turler, A., Gaggeler, H. W., Baltensperger, U.: Heterogeneous chemical processing of (NO_2)-N-13 by monodisperse carbon aerosols at very low concentrations. J. Phys. Chem. **100**(38), 15487–15493 (1996).
29. Murphy, D. M., Fahey, D. W.: Mathematical treatment of the wall loss of a trace species in denuder and catalytic-converter tubes. Anal. Chem. **59**(23), 2753–2759 (1987).
30. Mentel, T. F., Sohn, M., Wahner, A.: Nitrate effect in the heterogeneous hydrolysis of dinitrogen pentoxide on aqueous aerosols. Phys. Chem. Chem. Phys. **1**(24), 5451–5457 (1999).
31. Ammann, M., Cox, R. A., Crowley, J. N., Jenkin, M. E., Mellouki, A., Rossi, M. J., Troe, J., Wallington, T. J.: Evaluated kinetic and photochemical data for atmospheric chemistry: Volume VI - Heterogeneous reactions with liquid substrates. Atmos. Chem. Phys. **13**, 8045–8228 (2013).
32. Clegg, S. L., Brimblecombe, P., Wexler, A. S.: Thermodynamic model of the system H^+-NH_4^+-SO_4^{2-}-NO_3^--H_2O at tropospheric temperatures. J. Phys. Chem. A **102**(12), 2137–2154 (1998).
33. Zardini, A. A., Sjogren, S., Marcolli, C., Krieger, U. K., Gysel, M., Weingartner, E., Baltensperger, U., Peter, T.: A combined particle trap/HTDMA hygroscopicity study of mixed inorganic/organic aerosol particles. Atmos. Chem. Phys. **8**(18), 5589–5601 (2008).